POAC '99
Espoo, Finland

Proceedings of the 15th
International Conference on
Port and Ocean Engineering
under Arctic Conditions

NUMERICAL SIMULATION OF THE ICE FAILURE PROCESS

K. Shkhinek[1], S. Kapustiansky[1], A. Jilenkov[1] and T. Kärnä[2]

[1] St. Petersburg Technical University, St.Petersburg, Russia

[2] VTT Building Technology, Espoo, Finland

ABSTRACT

It is well-known that the edge of ice features has considerable roughness. Therefore, the contact between the structure and the ice feature develops within the small area. However, some methods of ice load determination assume that this contact is perfect and full. This simplifying assumption has significant influence on the ice load estimations, especially in theoretical investigations.

Numerical solution for the non perfect ice-structure contact has been developed. The model is used to simulate the failure of the ice edge in conditions when the ice sheet acts on the vertical-side structure. The ice edge roughness has been modelled by the tooth located at the ice edge and influence of this tooth on local and global loads has been analysed. The results of numerical experiments show that the global load increases and the local one decreases with the tooth width increase.

1. INTRODUCTION

Methods of ice loads determination are very often based on the assumption that ice/structure contact is perfect and contact area can be considered as a product of ice thickness and structure width. But in real conditions contact is never be perfect.

When ice approaches the structures its edge usually has certain roughness that can be considered as a set of local teeth. The results of observation of natural sea ice edges published by Takeuchi et al (1998) confirm the presence of significant initial roughness of the ice edge. Therefore during the first impact the ice edge can not be considered as a smooth, and in subsequent structure penetration (if velocity of penetration is not very small and creep does not develop) contact area is not perfect as well, because due to failure the ice edge develops into a wedge shape and contains both failured and intact ice. Therefore one can propose that usually ice pressure on the structure will be transferred through small teeth located in certain points of the contact area.

Loads that can be transferred through a limited contact area or a line-type contact were considered by Fransson (1991,1993), Joensuu and Riska (1989), Riska (1991),Tuhkuri (1991,1996). Laboratory experiments were carried out by Tuhkuri (1996), Gagnon (1995 a,b). Some full-scale observations were made by Takeuchi et al (1994), Takeuchi and Saeki (1995), (1998), Gagnon (1995), Timco and Frederking (1995), Frederking et al. (1990). All investigations show that when contact area decreases, pressure increases. This confirms importance of roughness consideration for ice loads calculation.

The idea to consider the edge roughness for calculation of loads on offshore structures was suggested and developed by Muhonen et al (1992) and Karna et al (1998). Karna worked out a computer program that considered ice sheet/ structure interaction. The ice sheet is divided into two zones - near the structure surface and far. All behaviour in near zone is determined by teeth interaction with the structure surface, failure, extrusion, etc. Stresses, arising in the near zone influence stress and strain fields in the far zone. Some parameters in Karna's model are taken from the experimental data, but some other (location of border between near and far zones, stress in a teeth, etc.) are based on certain assumptions and need more accurate determination.

This paper reflects the first step in Karna's model refinement. Special finite-difference computer program is developed. Only one tooth interaction with the structure and ice sheet is considered. Ice failure, local and global loads induced by this tooth interaction with the structure surface and approximate position of the border between near and far zones are investigated.

2. THE PROBLEM STATEMENT

2.1. Main equations

2D problem in vertical plane is considered. A semi-infinite ice sheet with thickness h moves with velocity v against a vertical wall. Velocity v should be not too low because creep is not considered. The sheet edge contains a single tooth that can be located at any level of the edge height. This tooth is a part of the ice sheet, its height is w and its length is l (Fig.1). Soft material can be located above and under the tooth. This material models property of the ice destroyed during previous interaction. It is characterised by modulus of deformation E. E/E_o ratio (E_o - modulus of deformation of the intact ice and E – one of the tooth), which can vary within the range $0 \le E/E_o \le 1$. Intact ice is elastic until failure criterion is reached. This criterion is used in the Coulomb-Mohr form. Material transits to the residual state after failure. In this state all failured material properties again are determined by Coulomb-Mohr law but with strength significantly lower than for the intact ice.

The main equations are written in the form:

Momentum equilibrium

$$\rho \frac{\partial v_i}{\partial t} = \frac{\partial \sigma_{ij}}{\partial x_j} \tag{1}$$

Constitutive equations:

$$\frac{\partial S_{ij}}{\partial t} = 2G(\dot{\varepsilon}_{ij} - \frac{1}{3}\dot{\varepsilon}H_{ij} - rS_{ij}) \tag{2}$$

$$\frac{\partial P}{\partial \tau} = -K(\dot{\varepsilon} - 2r\Lambda\tau) \tag{3}$$

where

$$\tau^2 = \frac{3}{8} S_{ij} S_{ij} \tag{4}$$

$$\dot{\varepsilon} = \dot{\varepsilon}_{kk} \quad (k=1,2,3) \tag{5}$$

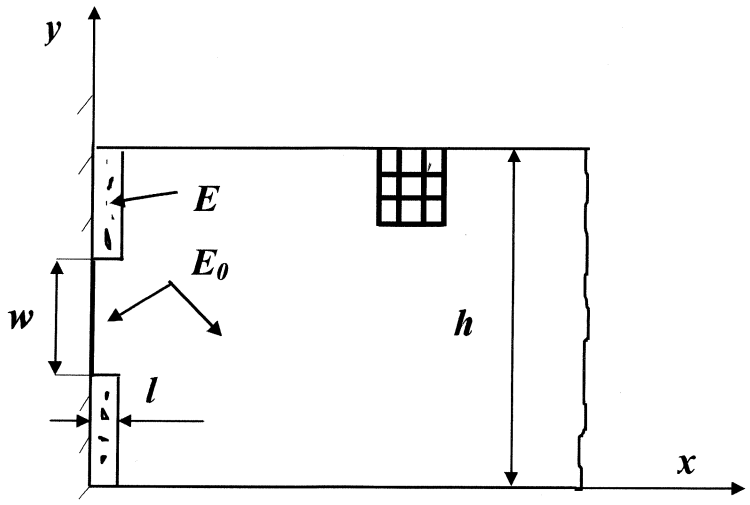

Figure 1. Scheme for design

Here x_1, x_2 – are axis of Cartesian system; summation over a repetitive index ($i,j=1,2$) is assumed; plane strain conditions are considered; dot above symbol represents time derivative ; v_i - velocity in direction i; G - shear modulus; K - bulk modulus; H_{ij} - Kroneker's function ($H=0$ if $i \neq j$, otherwise $H=1$); Λ - coefficient of dilatancy; r- scalar factor (determined from failure criterion (7)).

As it was mentioned above failure criterion is used in Coulomb-Mohr form that is shear failure will develop if

$$\sigma^f{}_{22} = -R_c + \sigma_{11} N \tag{6}$$

or $$S^f_{22} = -R_c + S_{11} N + (1-N)P \tag{7}$$

$$N = \frac{1+\sin\varphi}{1-\sin\varphi} \tag{8}$$

$$S_{ii} = \sigma_{ii} + P \tag{9}$$

$$P = -\frac{1}{3}\sigma_{kk} \qquad (k=1,2,3) \tag{10}$$

where σ_{11}, σ_{22} - are the maximal and the minimal principle stresses (compressive stresses are negative), R_c - unconfined strength, φ - angle of internal friction, P - pressure. Upper index f refers to parameters on the failure surface.

Tensile failure takes place if $\sigma_{11} = R_t$, where R_t - tensile strength. If both shear and tensile failure can arise simultaneously then Fridman's (1952) criterion

$$\left|\frac{\sigma_{22}}{\sigma^f_{22}}\right| > \frac{\sigma_{11}}{R_t} \tag{11}$$

is used. If Eq.(11) is true, then shear failure develops, otherwise - tensile one.

Boundary conditions are:

$\sigma_{xy} = \sigma_{yy} = 0$ if $y=0$ or $y=h$

$\sigma_{xy} = f\sigma_{xx}$ for $x=0$, $0 \le y \le h$

where f – friction coefficient.
Special boundary conditions were used at the far end of the sheet to avoid reflection of longitudinal and shear waves from this boundary. Investigations showed that during numerical modelling reflection was not registered and it was possible to continue computations over the long time period.

2.2. Method of solution

Finite-difference method and Whilkin's (1967) methodology are used for solution (Fig.1). The first application of this method to ice problems was discussed by Matskevitch and Shkhinek (1992). Nodes of the mesh are used for velocities calculation whereas stresses are determined in the centres of cells. 43 nodes are used through the sheet height. In horizontal direction the sheet length was divided on 200 cells.
The order of computation is the following:
a) all equations are rewritten in the finite-difference form;
b) velocity at each point of field is determined;
c) as velocities are known, elastic stresses can be computed from the constitutive equations;
d) failure criterions (by shear and tension) are checked in all points, if both of them happen in the same cell then equation (11) is used to choose the preferable criterion;
e) if shear failure will develop, then parameter l have to be determined.
From constitutive equations (2)-(3) in finite-difference form and condition (7) one can receive:

$$r = \frac{-S_{22}^{e} + S_{22}^{f}}{2\Delta t\left[G(NS_{11} - S_{22}) - K\Lambda\tau(1-N)\right]} \tag{12}$$

where

$$S_{22}^{f} = -R_c + NS_{11}^{e} + (1-N)P^{e}$$

Upper index e refers to values determined at elastic stage; Δt is time step. Parameters in denominator correspond to ones in the foregoing time moment.
New values of deviators are determined according to formula

$$S_{ij} = \frac{S_{ij}^{e}}{1 + 2Gr\Delta t} \tag{13}$$

New value of τ can be computed from equations (4) and (13) and new pressure is defined using formula

$$P = P^{e} + 2Kr\,\Lambda\tau\Delta t \tag{14}$$

If tensile failure takes place, then new stress values are determined by formula:

$$\sigma_{11} = R_t \tag{15}$$

and other stresses are defined by formulas (Mainchen and Sak, 1967) that is

$$\sigma_{22} = \sigma_{22}^{e} - (\sigma_{11}^{e} - R_t)\frac{\lambda}{\lambda + 2G} \tag{16}$$

$$\sigma_{33} = \sigma_{33}^{e} - (\sigma_{11}^{e} - R_t)\frac{\lambda}{\lambda + 2G} \tag{14}$$

where λ - Lame's coefficient.

Later velocity field should be recalculated and the whole process repeated. So, this method gives opportunity to investigate failure process development in time and in space.

3. RESULTS OF COMPUTATION

The following results refer to the situation when the tooth is located at the centre of the ice sheet cross section. The following parameters $E/E_0 = 0.05$, $f=0$, $w/h=0.1$, $E_0 = 8GPa$, $R_C=0.7MPa$, $\phi=20°$, $\Lambda=0$ were mainly used in computations.

3.1. Load history and failure pattern

The non-dimensional load $\bar{F} = F / R_c h$ history for $w/h=0.1$, $R_t/R_c=0.3$ is shown in Fig.2.

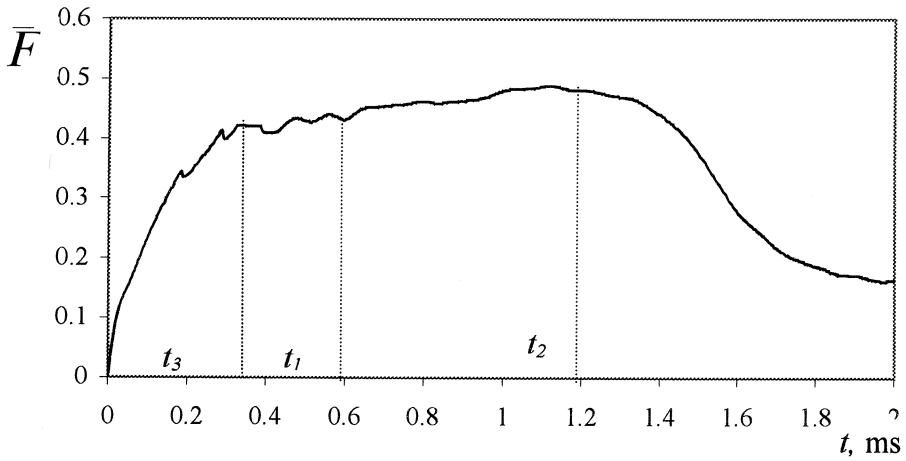

Figure 2. Load history
$w/h=0.1$, $R_t/R_c=0.3$, $E/E_o=0.05$, $v=0.2$ m/s, $f=0$

a) b)

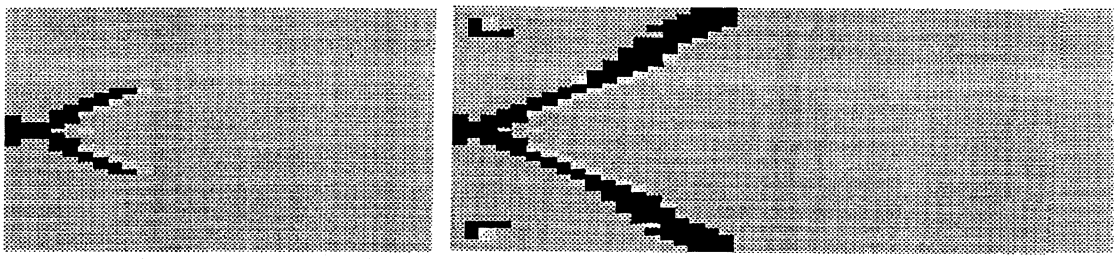

Figure 3. Failure development
a) $t=0.605$ ms, b) $t=1.25$ ms
$R_t/R_c=0.3$, $w/h=0.1$, $E/E_o=0.05$, $v=0.2$ m/s

Failure patterns at the time instants t_1 and t_2 are presented in Fig.3.a,b, and velocity field corresponding to the same moments in Fig.4.a,b. In Fig.3 cells failured by shear are presented as dark points whereas ones failured by tension are lighter. Velocity vectors can be seen in Fig.4.a,b. Each arrow in this figure reflects both velocity amplitude and direction. Figures demonstrate failure development and shows that maximal load corresponds to time moment when triangles near the sheet edge form. Later these particles are separated from the sheet by failured zone and begin to fly off. The next stage – fly-away process was not considered in computations. After triangles formation load decreases. Analysis of local pressure history in the section corresponding to the centre of the sheet ($y=0.5h$) shows, that the maximal pressure takes place significantly earlier than the maximal load (in Fig.2 it corresponds to the time instant t_3).

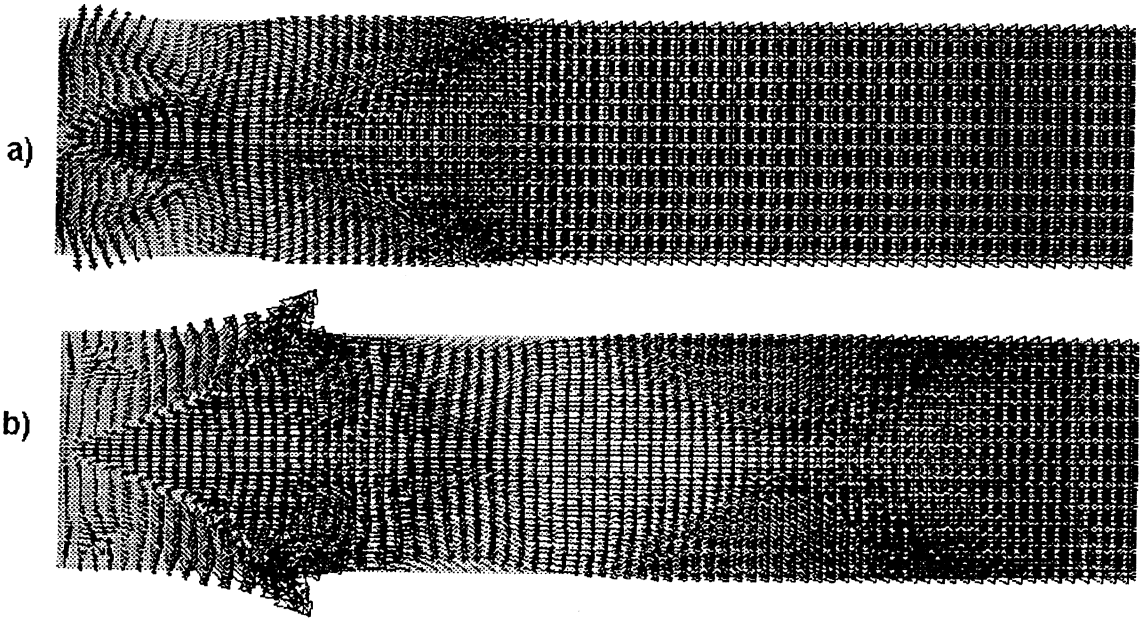

Figure 4. Velocity field in the sheet for the input data used in Figure 3 for approximately the same time moments.

Failure pattern significantly depends on the R_t/R_c ratio and methods of description of material properties. In particular, different pattern was observed for $R_t/R_c=0.3$, 0.2 and 0.1 (compare Fig. 3, 4 and.5.) at the time moment corresponding to the maximal load.

One can see that velocity fields in Fig.4 and Fig.5c have almost opposite direction. In Fig.4 triangles move away from the structure and it is possible to suppose that extrusion will not induce additional loading. In Fig.5c destroyed particles move against the structure and probably extrusion consideration will lead to increase of the maximal load. If extrusion is not considered then the maximal load in these numerical experiments slightly depends on R_t/R_c ratio, bur failure zones do depend.

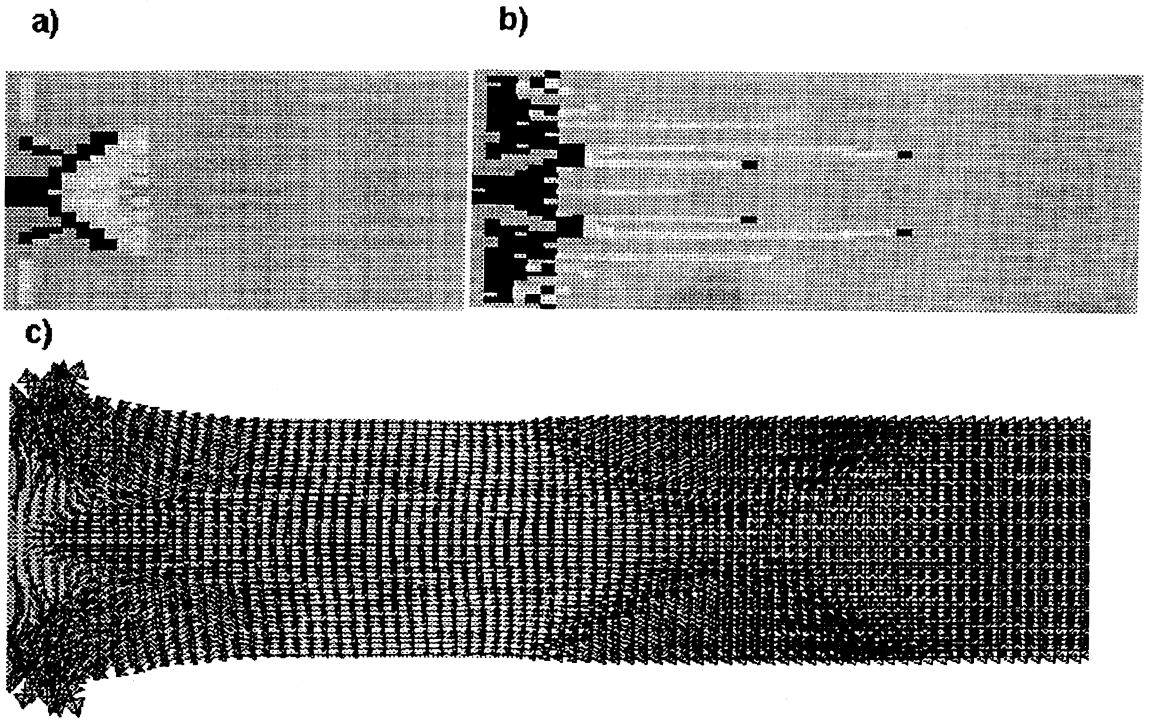

Figure 5. Failure pattern and velocity field
a) $R_t/R_c=0.2$, $w/h=0.1$, $E/E_o=0.05$, $v=0.2$ *m/s*
b),c) $R_t/R_c=0.1$

3.2. The tooth width and length.

The tooth width significantly influences local stress and global load. The maximal normal stress distribution across the section $x=0$ is shown in Fig.6. One can see that for the narrow tooth the maximal pressure to unconfined strength ratio is about 2.1.

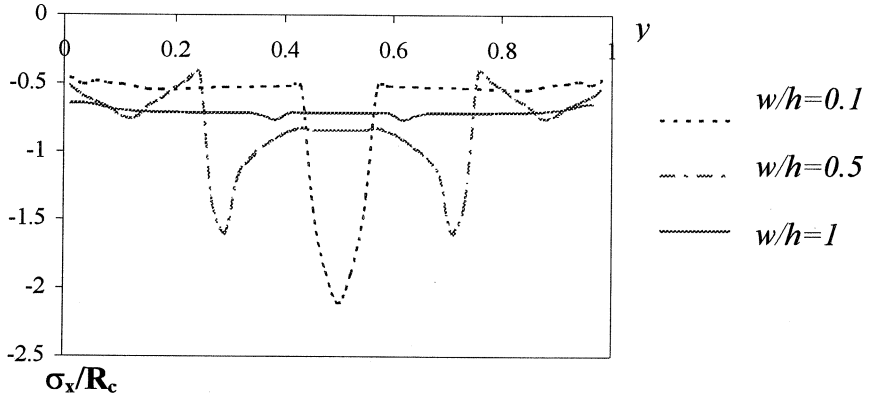

Figure 6. Stress distribution along the cross-section $x=0$
$R_t/R_c=0.3$, $w/h=0.1$, $E/E_o=0.05$, $v=0.2$ *m/s*

It should be mentioned that approximately the same value was received in Takeuchi's and Saeki's (1995) experiments (see Table 4 of this work). The reason of this phenomenon – confinement of the tooth by the sheet along the line x=*0*.

If tooth length *l* increases then the influence of confinement along the line x=*0* on the strength of the whole tooth material is less and the maximal stress decreases .Dependence received in this work is resemble to one received in Tuhkuri(1993) experiments (Fig 4 of his work)

There is great difference in stress distribution along the *y* axis for different tooth widths. If *w/h=0.1* then the maximal stress corresponds to central section of the sheet. In other situations the maximal stress concentration approximately coincides with the tooth corners. The maximal local stresses ratio induced by narrow tooth to those corresponding to smooth ice edge can be as large as 3. In spite of the greatest local pressure is induced by narrow tooth, global load, corresponding to this situation is lower than one for wide tooth. It can be seen in Fig.7, where local stress σ_x / R_c and global non-dimensional load $\bar{F}$ versus w/h dependencies are demonstrated (it is necessary to emphasise that these data refer to condition $E/E_0=0$, when the tooth without surrounding soft material is considered).

Loads for different tooth widths can be perfectly characterised by formula

$$\frac{F_1}{F_2} = \left(\frac{w_1}{w_2}\right)^{0.7}$$

where F_1 and F_2 - load, corresponding to tooth width w_1 and w_2, accordingly.

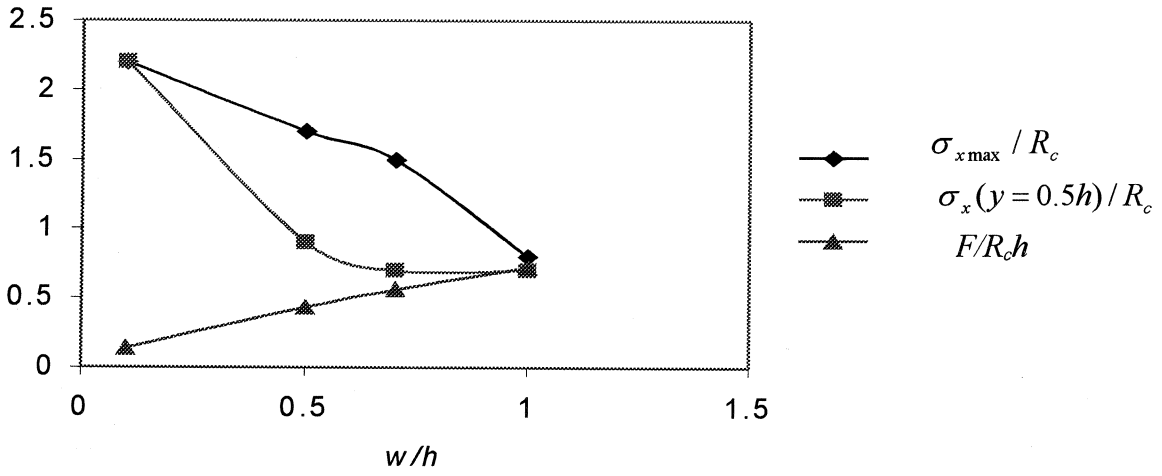

Figure 7. Stress and load dependence on *w/h*

$R_t/R_c=0.3$, $E/E_o=0$, $v=0.2$ *m/s*

3.3. The border between near and far zones

The maximal stress in time σ_x along the central line ($y=0.5h$) has extremum at the small distances from the tooth and decreases to the certain level far from the tooth. We assumed the distance where the maximal stress σ_x begins to be more or less constantly distributed along

the line $y=0.5h$ to be a border between near and fare zones. In majority of cases (not for a very wide tooth) this value is approximately equal to the ice thickness, but if $w=h$, it can increase up to $(2\text{-}3)h$.

CONCLUSIONS

Significant ice edge roughness is a reality that should be taken into account while determining ice loads. The existence of the irregularities influences local pressure, global loads and failure pattern. The narrower is the irregularity , the larger is the local pressure and the smaller is the global load.

In this work different assumptions were made about the properties of ruptured material. These assumptions do not influence the maximal stress, weakly influence the maximal load, but can noticeably influence failure pattern. This fact demonstrates that for the investigation of the failure pattern one has to know accurately all ice properties Extrusion process and friction along the structure surface were not considered yet and probably they will significantly influence the results.

ACKNOWLEDGMENT

Authors would like to gratify INTAS Committee and participants of LOLEIF project for the support of this work.

REFERENCES

Fransson, L., Stehn, L. 1993. Porosity Effects on Measured Strength of Warm Ice. Proceedings of POAC Conference, Vol.1, pp.23-37.

Fransson,L., Olofsson,T., Sandkvist,J. (1991). Observation of the Failure Process in Ice Blocks Crushed by a Flat Indentor. Proceedings of the POAC Conf.1991 vol. 1. pp501-514/

Frederking, R.M.W., Jordaan, I.Y., McCallum, J.S. (1990). Field Tests of ice Indentation of Medium Scale Hobson's Choice Ice Island, 1989. Proceedings of the IAHR Symp. Vol. II Pp 931-944

Fridman, J.B. 1952. Mechanical Properties of Metals. Moscow, 350p. (in Russian).

Gagnon, R.E. (1994a). Generation Of Melt During Experiments on the Freshwater Ice. Cold Regions Science And Technology, Vol. 22 N 4, Pp. 385-398

Gagnon, R.E. (1994b). Melt Lager Thickness Measurements During Crushing Experiments on the Freshwater Ice. Journal of Glaciology, Vol. 4, Pp. 119-124

Gagnon, R.E. (1995). Analysis from Visual Data from Medium Scale Indentation Experiments at Hobson's Choice Ice Island., Cold Regions Science and Technology, Vol. 28, Pp. 45-58

Joensuu, A., Riska, K. 1989. Contact Between Ice and a Structure. ESPOO, Helsinki University of Technology, Ship Laboratory, Report M-88, 57 p. (In Finnish).

Journal of Offshore and Polar Engineering, Vol.5, N4, pp.279-285.

Karna, T., Kamesaki, K., Tsukuda H., 1998. A Layered Flaking Model of Ice-Structure Interaction. Proceedings of International Symposium on Ice, Vol.1, pp.575-582.

Mainchen, J., Sak, S. 1967. Method 'Tensor'. (Translation into Russian). In the book 'Fundamental Methods in Hydrodynamics', Vol.3, Academic press, New York and London, 1964.

Matskevitch, D.G., Shkhinek, K.N. 1992. A Computer-Based Simulation of the Ice Fracture near a vertical pile. International Journal of Offshore and Polar Engineering, 2: p.123-128.

Muhonen, A., Karna, T., Eranti, E, Riska, K., Jarvinen, E., Lehmus, E. 1992.Laboratory Indentation Tests with Thick Freshwater Ice. VTT Research Notes, 1370: 92-106.

Riska, K. (1991) Medium-Scale Ice-Structure Interaction :Failure Zone Characterisation. Proceedings of the POAC Conference 1991 vol. 1,pp 126-140

Takeuchi, T., Saeki, H. 1995. Indentation Pressure in Ice/Vertical Structure Interaction.

Takeuchi, T., Saeki, H., Okamado, S., Yamashita, T. 1994. Effect of Imperfect Contact on Total Ice Force. Proceedings of the Fourth ISOPE Conference, Vol.2., pp.509-513.

Takeuhi, T., Saeki, H. 1998. Significance of Ice Sheets Leading - Edge Roughness in Relation to Ice Load. Journal of Offshore and Polar Engineering, Vol.8, N3, pp.161-166.

Timco, G.W. and Frederking, R.M.W. (1995) Experimental Investigations Of The Behaviour Of Ice At The Contact Zone. Mech. of Geomaterial Surfaces. A.R.S. Chelvaduray And A.G. Boilon Editors, pp 35-55

Tuhkuri, J. (1996). Experimental Investigations and Computational Fracture Mechanics Modelling of Brittle Ice Fragmentation. Acta Polytechnica Scandinavica, Mech.Eng.Series, 120: 105p.

Tukhuri ,J. (1993) Laboratory Investigations of Ice-Structure Contact. Proceedings of the POAC Conference1993,vol 2,pp617-627.

Wilkins, M.L. (1967). Computation of Elastic-Plastic Yielding. (Translation into Russian). In the book 'Fundamental Methods in Hydrodynamics', Vol.3, Academic press, New York and London, 1964.